

SANDIA REPORT

SAND93-0188 • UC-905

Unlimited Release

Printed September 1993

Microfilm

Evaluating the Ignition Sensitivity of Thermal Battery Heat Pellets

Edward V. Thomas



8595269

Prepared by
Sandia National Laboratories
Albuquerque, New Mexico 87185 and Livermore, California 94550
for the United States Department of Energy
under Contract DE-AC04-76DP00789

SANDIA NATIONAL
LABORATORIES
TECHNICAL LIBRARY

Issued by Sandia National Laboratories, operated for the United States Department of Energy by Sandia Corporation.

NOTICE: This report was prepared as an account of work sponsored by an agency of the United States Government. Neither the United States Government nor any agency thereof, nor any of their employees, nor any of their contractors, subcontractors, or their employees, makes any warranty, express or implied, or assumes any legal liability or responsibility for the accuracy, completeness, or usefulness of any information, apparatus, product, or process disclosed, or represents that its use would not infringe privately owned rights. Reference herein to any specific commercial product, process, or service by trade name, trademark, manufacturer, or otherwise, does not necessarily constitute or imply its endorsement, recommendation, or favoring by the United States Government, any agency thereof or any of their contractors or subcontractors. The views and opinions expressed herein do not necessarily state or reflect those of the United States Government, any agency thereof or any of their contractors.

Printed in the United States of America. This report has been reproduced directly from the best available copy.

Available to DOE and DOE contractors from
Office of Scientific and Technical Information
PO Box 62
Oak Ridge, TN 37831

Prices available from (615) 576-8401, FTS 626-8401

Available to the public from
National Technical Information Service
US Department of Commerce
5285 Port Royal Rd
Springfield, VA 22161

NTIS price codes
Printed copy: A03
Microfiche copy: A01

EVALUATING THE IGNITION SENSITIVITY OF THERMAL BATTERY HEAT PELLETS

Edward V. Thomas
Department 323
Sandia National Laboratories

ABSTRACT

Thermal batteries are activated by the ignition of heat pellets. If the heat pellets are not sensitive enough to the ignition stimulus, the thermal battery will not activate, resulting in a dud. Thus, to assure reliable thermal batteries, it is important to demonstrate that the pellets have satisfactory ignition sensitivity by testing a number of specimens.

There are a number of statistical methods for evaluating the sensitivity of a device to some stimulus. Generally, these methods are applicable to the situation in which a single test is destructive to the specimen being tested, independent of the outcome of the test. In the case of thermal battery heat pellets, however, tests that result in a nonresponse do not totally degrade the specimen. This peculiarity provides opportunities to efficiently evaluate the ignition sensitivity of heat pellets. In this paper, a simple strategy for evaluating heat pellet ignition sensitivity (including experimental design and data analysis) is described. The relatively good asymptotic and small-sample efficiencies of this strategy are demonstrated.

KEY WORDS: Censored Data; Experimental Design; Maximum Likelihood Estimation; Sensitivity Testing.

1. INTRODUCTION

Sensitivity testing involves the characterization of a response curve that relates the stimulus level applied to a specimen with the probability of a *response*. This situation arises in many fields of research from biological assays (e.g., see Finney 1978) to the testing of explosives (e.g., see Dixon and Mood 1948). The outcome of an experiment on an individual specimen is dichotomous (e.g., response/nonresponse, explode/not explode, die/survive). A number of methods for obtaining and analyzing sensitivity test data have appeared in the statistical literature (e.g., see Dixon and Mood 1948, Robbins and Monro 1951, and Wu 1985).

A response curve is estimated by conducting a series of experiments in which the stimulus level is varied. The recorded outcome of each experiment is whether or not a response to the stimulus occurred. Often, the 50th percentile of the response curve is of interest (in biological studies involving the dichotomous outcome, die/survive, this percentile is referred to as the LD50). Usually, experiments are performed sequentially so that results from previous experiments can be used to select the stimulus level associated with the current experiment. The experimental results can be compactly summarized by $(S_1, I_1), (S_2, I_2), \dots, (S_n, I_n)$, where S_i is the stimulus level applied to the specimen used in the i^{th} experiment, and I_i is an indicator of the outcome of the i^{th} experiment.
 $I_i = 1$ (0) if the specimen used in the i^{th} experiment did (did not) respond to S_i .

Experimental design in this situation, consists of choosing n (the number of experiments to run), S_1 (the stimulus applied to the first specimen), and the logic used to select S_2, S_3, \dots, S_n . In the up-and-down (or Bruceton) method, proposed by Dixon and Mood (1948) the logic used to select stimulus levels is,

$$\begin{aligned} S_{i+1} &= S_i + \Delta & \text{if } I_i = 0 \\ S_i - \Delta & & \text{if } I_i = 1, \text{ where} \end{aligned}$$

Δ is a fixed step size of the stimulus. This method can be effective if the purpose is to estimate the 50th percentile of the response curve. For small to moderate values of n , the performance of this method depends on good guesses for S_1 and Δ . Other methods of selecting the S_i , such as the stochastic approximation method (Robbins and Monro 1951), are more general and can be used to estimate arbitrary percentiles of the response curve. In general, an experimental strategy should be selected based on the objectives of the study, previous data, and a conceptual model. In addition, a strategy should be tailored to take advantage of the uniqueness of the specific application as well as to facilitate the resulting data analysis.

1.1 Thermal Batteries

A thermal battery consists of a number of electrochemical cells stacked together in series to achieve the desired output voltage. A cross-sectional representation of a typical thermal cell is shown in Figure 1. Each cell assembly consists of an anode, electrolyte mixed with a metal-oxide binder, cathode, and pyrotechnic mixture (Fe/KClO_4), all in pellet (or disk) form in the solid state. A thermal battery can remain dormant (and preserved) for many years and will not deliver its power until its internal temperature is elevated above the melting point of the electrolyte. Temperature elevation is achieved by the ignition of the Fe/KClO_4 heat pellets. Thermal batteries are used in a number of military and space applications when there is a need for a relatively long dormant lifetime with a large power requirement and a short activation time (see Vincent et al. 1984).

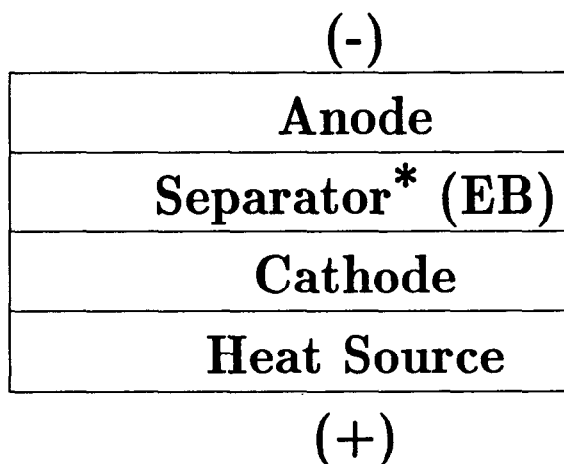


Figure 1- Cross-sectional Representation of a Pelletized Thermal Cell
*Separator contains electrolyte (E) immobilized with MgO binder (B)

The performance of thermal batteries can be affected by the ignition sensitivity of the heat pellets. Ignition sensitivity is determined by the energy per unit area required to ignite a heat pellet and is assumed to be a homogeneous quantity throughout a pellet. If the heat pellets are not sensitive enough to the energy stimulus, the thermal battery will not activate, resulting in a dud. Thus, to assure reliable thermal batteries, it is important to demonstrate that the pellets have satisfactory ignition sensitivity. This is generally accomplished through a lot sampling program in which a number of pellets are randomly selected and tested. The response curve (or selected percentiles) can be estimated for the lot based on the experimental results and subsequent analysis.

Individual heat pellets are tested for ignition sensitivity by using a laser (see Figure 2). Coherent light from the laser, originally at an energy intensity of E_0 , is directed through a series of up to four absorbing filters where the energy intensity is attenuated to a level E . This energy is directed onto a spot within one of six sectors on the pellet (see Figure 3). If the energy density is sufficient, the pellet ignites rapidly and is destroyed. Otherwise, the spot is charred, but the pellet

does not ignite. Once charred, the sector cannot be retested. Other sectors, however, can be tested. Therefore, tests that result in a nonresponse do not degrade the other sectors of the specimen. This peculiarity provides the opportunity to evaluate the ignition sensitivity of heat pellets in an efficient manner. Thus, the purpose of this paper is to put forth a method for experimental design and data analysis for this situation.

The remainder of this paper is organized as follows. Section 2 provides more details associated with battery pellet testing; including objectives, procedures, and modeling. In Section 3, a sequential testing strategy is proposed. Section 4 illustrates how the proposed procedure can be represented as a Markov Chain. This representation is utilized in the derivation of the asymptotic performance of the proposed method, which is presented in Section 5. A small Monte Carlo study is used to illustrate the small-sample performance of the proposed method in Section 6. A short conclusion follows.

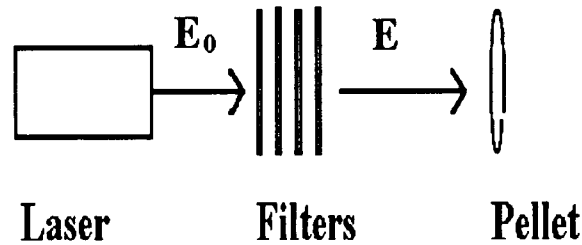


Figure 2 - Attenuation of Laser Source Through Filters

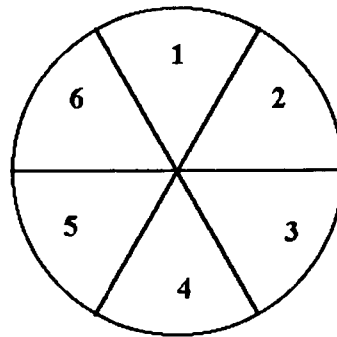


Figure 3 - Plan View of Heat Pellet (Disk)

2. RESPONSE MODEL AND TESTING

The threshold energy needed to ignite a pellet varies somewhat from pellet to pellet and lot to lot. Analyses of historical data suggest the probit model,

$$\text{Prob}\{\text{Ignition} \mid \text{Stimulus} = S\} = \Phi\left(\frac{S - \mu}{\sigma}\right),$$

provides a good approximation to the distribution of threshold energies within a lot. Earlier test data from many production lots indicate that μ and σ , which are the parameters of interest, are likely to be in the following regions; .4 to .9 Joules for μ , and .05 to .2 Joules for σ . Production engineers are interested in estimating the 50th and 90th percentiles of the threshold energy distribution for each lot at relatively small expense. It is not necessary to resolve μ outside the range of interest as pellets with ignition sensitivities outside that range are unacceptable. The production engineers need simple methods for both the design of the sensitivity experiment and the subsequent analysis.

In addition to using the sensitivity testing for lot acceptance, production personnel want to use control charts of the estimates of μ and σ to help monitor the production process. Also, the parameter estimates can be used as response variables in experiments to gauge the effect on ignition sensitivity of the three major process factors during the fabrication of heat pellets: composition, particle size of Fe, and compaction pressure. Briefly, the process consists of pressing a mixture of iron and potassium perchlorate powders into pellets (disks) to a specified density for a given diameter, thickness, and mass.

During testing, a technician selects up to four filters (out of a set of seven filters) to place between the laser source and the target. The laser is then fired. The energy delivered to the spot on the pellet is $E = (E_0 + \delta_f) \prod_{k \leq 4} \rho_k$, where δ_f is a random disturbance that perturbs the nominal laser output (during the f^{th} firing) and ρ_k (≤ 1) determines the attenuation due to the k^{th} filter that is used. The laser output, $E_0 + \delta_f$, is measured with relatively little error during each laser firing. The attenuation factors, ρ_k , are known for each filter. There are $\binom{7}{4} + \binom{7}{3} + \binom{7}{2} + \binom{7}{1} = 98$ possible filter combinations; each yields a unique overall attenuation factor, $\prod_{k \leq 4} \rho_k$.

Knowledge of the testing costs is an integral part of designing an economically efficient experiment. We will discuss this only in relative terms here. Although the pellets are relatively inexpensive, there is significant manpower expense in performing the test. There is relatively little time and effort required to mount the heat pellet, prepare the laser, and to change filters. However, if the pellet ignites, it is necessary and relatively expensive (with regard to time and effort) to clean residue from the optical path of the test apparatus in order to prepare for the next pellet. Therefore, it seems that a prudent experimental strategy should rely on extensive testing of each of a relatively small number of pellets, rather than a modest amount of testing on each of a

relatively large number of pellets.

3. EXPERIMENTAL STRATEGY

Part of the experimental design consists of selecting the filter combinations that span the region of interest. From knowledge of E_0 and the attenuation factors, one can compute the delivered energy that can be expected, $E_0 \cdot \prod_{k \leq 4} \rho_k$, by using various combinations of filters. Fourteen of these filter combinations form a set that is well spread out and spans the region of interest. The expected energy values (in Joules) corresponding to these 14 combinations of filters are given by $R = \{R_1, R_2, \dots, R_{14}\} = \{.400, .450, .495, .555, .589, .620, .672, .707, .757, .802, .845, .894, .957, 1.00\}$. Although we have limited the number of filter combinations to 14, we still have a great deal of flexibility in specifying which of the 14 stimulus levels is to be used for a given test.

The algorithm proposed to specify the stimulus level is a variation of the up-and-down method that utilizes the ability to retest a pellet if it doesn't ignite. To generalize this for other than 14 candidate stimulus levels, but for the situation of six potential firing attempts per pellet, assume that there are $L(\text{even}) \geq 6$ discrete expected stimulus levels possible. The specified stimulus level associated with the j^{th} test of the i^{th} pellet is given by S_i^j . Like the up-and-down method, this algorithm specifies that the $i + 1^{\text{st}}$ pellet is initially tested at a level, S_{i+1}^1 , dictated by the results obtained from the i^{th} pellet. For subsequent tests of a pellet, the stimulus is advanced one level at a time until the pellet ignites or all six sectors are tested. The proposed algorithm used to specify stimulus levels, followed by a brief narrative, is given on the next page.

Algorithm Used to Specify Stimulus Levels

```
INIT:      stind  $\leftarrow \frac{L}{2} + 1$ ;  
           i  $\leftarrow 0$ ;  
NXTPEL:   REPEAT UNTIL (i = n);  
           i  $\leftarrow i + 1$ ;  
           j  $\leftarrow 1$ ;  
           stind  $\leftarrow \min\{\max\{\text{stind} - 3, 1\}, L - 5\}$ ;  
            $S_1^j \leftarrow R_{\text{stind}}$ ;  
           IF PELLET IGNITES THEN GO TO NXTPEL;  
           REPEAT UNTIL (j = 6);  
           j  $\leftarrow j + 1$ ;  
           stind  $\leftarrow \text{stind} + 1$ ;  
            $S_1^j \leftarrow R_{\text{stind}}$ ;  
           IF PELLET IGNITES THEN GO TO NXTPEL;  
           end;  
           end;
```

Begin by testing one sector of the first pellet at stimulus level $R_{\frac{L}{2}+1}$ (the stimulus level index, “stind”, is $\frac{L}{2} + 1$). If $L = 14$, $S_1^1 = .589$ Joules. If the pellet does not fire, then advance the stimulus one level and test the next sector of the pellet (i.e., “stind \leftarrow stind + 1” so that $S_1^2 = R_{\frac{L}{2}+2}$). Repeat this until the pellet ignites or until all six sectors of the pellet are used. Generally, the initial testing level of a pellet, S_1^1 , is three levels lower than the highest level at which the previous pellet was tested. This is meant to *center* the testing window about the point at which the last pellet ignited. However, this rule is not hard and fast for two reasons. First, testing cannot begin at a level below R_1 . Second, there is no benefit to beginning the test above R_9 , as there are up to six possible stimulus levels that can be used. The logic “stind $\leftarrow \min\{\max\{\text{stind} - 3, 1\}, L - 5\}$ ” is used to handle these contingencies. Otherwise, the logic is very straightforward and easy to use. Table 1 illustrates, with simulated test results, how the proposed algorithm works.

Table 1 - Proposed Algorithm Illustrated With Simulated Test Results
I = Ignition N = No Ignition

Expected Energy Level (Joules)									
Pellet	.495	.555	.589	.620	.672	.707	.757	.802	.845
1			N	N	N	N	N	I	
2					I				
3		N	N	I					
4	N	N	N	N	N	N			
5			N	N	N	N	N	I	
6					N	N	N	N	I
7						I			
8			N	N	N	N	N	I	
9					N	N	N	N	I
10						I			
.									
.									
.									

It is relatively straightforward to summarize these test results. For each pellet, the threshold energy levels are either right, left, or interval censored. To simplify the discussion, suppose that the nominal laser output is not disturbed (i.e. $\delta_f = 0$). Then, by deduction, the threshold energy level of the first pellet is censored in the interval [.757, .802] Joules. The threshold energy associated with the second pellet is left-censored with a limit of .672 Joules. The threshold energy associated with the fourth pellet is right-censored with a limit of .707 Joules. For 14 stimulus levels, one can list 31 possible outcomes (Of course the number of outcomes grows to infinity when we let δ_f vary randomly). Nine outcomes involve left-censored energy thresholds, nine involve right-censored thresholds, and thirteen involve interval-censored thresholds. See Table 2 in Section 4 for an enumeration of those outcomes. The probability of each of these outcomes, denoted by $O = \{O_1, O_2, \dots, O_{31}\}$, depends on μ and σ which will be estimated by maximum likelihood. The efficiency of maximum likelihood estimation used in conjunction with the proposed experimental strategy will be discussed in Sections 5 and 6. As a preliminary step, we will consider some of the properties of the experimental strategy which, in one sense, can be represented as a Markov Chain.

4. MARKOV CHAIN REPRESENTATION OF PROPOSED METHOD

To analyze the performance of the proposed method insofar as estimating μ , and σ , it is useful to represent the process that arises from the proposed method as a Markov Chain. A Markov Chain is a random process which at any stage is in one of a number of states, and which advances to another state at the next stage with a probability that is dependent on the state of the previous stage, but on no earlier stage (see e.g., Isaacson and Madsen, 1976). In the case of battery

pellet testing, we will use this representation to obtain the probability of each of the 31 possible outcomes (again, we will assume that $\delta_f = 0$). The state of the process will be associated with the initial stimulus that is applied to each pellet. Let X_i be the state of the process associated with testing of the i^{th} pellet. $X_i \in \{1, 2, \dots, 9\}$ indicates which of the nine permitted initial stimulus levels $\{R_1, R_2, \dots, R_9\}$ is applied to the i^{th} pellet. For instance, if $S_1^1 = .400$ Joules, then $X_1 = 1$. The transition probability, $P_{J,K} = \text{Prob}\{X_{i+1} = K \mid X_i = J\}$, is the conditional probability that the $i+1^{\text{st}}$ pellet will be initially tested at the R_K^{th} stimulus level, given that the i^{th} pellet was initially tested at the R_J^{th} level.

These transition probabilities depend on the model parameters, μ and σ , and will henceforth be written as $P_{J,K}(\mu, \sigma)$. For instance, $P_{1,1}(\mu, \sigma) = \Phi\left(\frac{.555 - \mu}{\sigma}\right)$. That is, we will begin testing the $i+1^{\text{st}}$ pellet at .400 Joules only if the i^{th} pellet ignited at an energy level at or below .555 Joules. Now suppose that $X_i = 5$ (i.e., $S_i^1 = R_5 = .589$ Joules). In this case, $P_{5,1}(\mu, \sigma) = 0$, as it is impossible to begin testing of a new pellet at more than three levels below where testing began for the previous pellet. An example of a complete transition probability matrix is

$$P(.7, .1) = \begin{bmatrix} .074 & .060 & .866 & 0 & 0 & 0 & 0 & 0 & 0 \\ .074 & .060 & .078 & .788 & 0 & 0 & 0 & 0 & 0 \\ .074 & .060 & .078 & .178 & .610 & 0 & 0 & 0 & 0 \\ .074 & .060 & .078 & .178 & .138 & .472 & 0 & 0 & 0 \\ 0 & .134 & .078 & .178 & .138 & .188 & .284 & 0 & 0 \\ 0 & 0 & .212 & .178 & .138 & .188 & .130 & .154 & 0 \\ 0 & 0 & 0 & .390 & .138 & .188 & .130 & .080 & .074 \\ 0 & 0 & 0 & 0 & .528 & .188 & .130 & .080 & .074 \\ 0 & 0 & 0 & 0 & 0 & .716 & .130 & .080 & .074 \end{bmatrix}.$$

The Markov Chain representation can be used to compute the stationary distribution (large n) of the X -process which is given by

$$\boldsymbol{\Pi}(\mu, \sigma) \text{ is any row of } \mathbf{W} = \lim_{s \rightarrow \infty} \mathbf{P}(\mu, \sigma)^s.$$

For example, we find that

$$\boldsymbol{\Pi}(.7, .1) = (.031, .051, .119, .216, .199, .218, .107, .047, .012).$$

$\boldsymbol{\Pi}$ gives the long-term probabilities that the process is in each of the nine possible states. Therefore, for example, when $\mu = .7$ and $\sigma = .1$, the long-term probability that the process is in the first state is about .031. Note that these long-term probabilities are independent of where the process starts.

Π can then be used to describe the long-term distribution (large n) of the set of 31 possible outcomes. To describe this distribution, we will let

$$P_{\infty}(O_m; \mu, \sigma) = \lim_{i \rightarrow \infty} \text{Prob} \left\{ \text{Testing of the } i^{\text{th}} \text{ pellet yields outcome } O_m \right\}.$$

It is straightforward to show that

$$P_{\infty}(O_m; \mu, \sigma) = \sum_{J=1}^9 \Pi_J(\mu, \sigma) \cdot \text{Prob}\{O_m | X = J; \mu, \sigma\}, \text{ where}$$

$\Pi_J(\mu, \sigma)$ is the long-term probability of the process being in the J^{th} state and is the J^{th} element of $\Pi(\mu, \sigma)$ and $\text{Prob}\{O_m | X = J; \mu, \sigma\}$ is the probability that we observe outcome O_m given the process is in the J^{th} state. Table 2 gives the long-term distribution of the outcomes for five combinations of μ and σ that are in the region of interest.

Table 2 - $P_{\infty}(O_m; \mu, \sigma)$ for selected values of μ and σ

ID	Outcome	$\mu=.7$ $\sigma=.1$	$\mu=.6$ $\sigma=.05$	$\mu=.6$ $\sigma=.2$	$\mu=.8$ $\sigma=.05$	$\mu=.8$ $\sigma=.2$
O ₁	Y ≤ .400	.0000	.0000	.0511	.0000	.0005
O ₂	Y ≤ .450	.0003	.0003	.0241	.0000	.0010
O ₃	Y ≤ .495	.0024	.0054	.0703	.0000	.0044
O ₄	Y ≤ .555	.0159	.0442	.0499	.0000	.0104
O ₅	Y ≤ .589	.0266	.0163	.0536	.0000	.0187
O ₆	Y ≤ .620	.0462	.0030	.0307	.0000	.0366
O ₇	Y ≤ .672	.0416	.0000	.0195	.0017	.0349
O ₈	Y ≤ .707	.0257	.0000	.0077	.0102	.0442
O ₉	Y ≤ .757	.0087	.0000	.0040	.0288	.0785
O ₁₀	Y > .620	.0242	.0606	.1483	.0000	.0190
O ₁₁	Y > .672	.0315	.0176	.0382	.0000	.0194
O ₁₂	Y > .707	.0560	.0049	.0695	.0000	.0467
O ₁₃	Y > .757	.0614	.0002	.0262	.0022	.0550
O ₁₄	Y > .802	.0307	.0000	.0175	.0117	.0636
O ₁₅	Y > .845	.0160	.0000	.0063	.0313	.0816
O ₁₆	Y > .894	.0028	.0000	.0022	.0100	.0427
O ₁₇	Y > .957	.0002	.0000	.0004	.0003	.0298
O ₁₈	Y > 1.00	.0000	.0000	.0001	.0000	.0300
O ₁₉	.400 < Y ≤ .450	.0001	.0002	.0219	.0000	.0004
O ₂₀	.450 < Y ≤ .495	.0011	.0068	.0314	.0000	.0012
O ₂₁	.495 < Y ≤ .555	.0107	.1190	.0737	.0000	.0055
O ₂₂	.555 < Y ≤ .589	.0250	.2188	.0526	.0000	.0075
O ₂₃	.589 < Y ≤ .620	.0483	.2414	.0554	.0000	.0131
O ₂₄	.620 < Y ≤ .672	.1429	.2222	.0636	.0010	.0397
O ₂₅	.672 < Y ≤ .707	.1186	.0346	.0350	.0139	.0373
O ₂₆	.707 < Y ≤ .757	.1477	.0044	.0266	.1393	.0650
O ₂₇	.757 < Y ≤ .802	.0761	.0000	.0129	.3202	.0702
O ₂₈	.802 < Y ≤ .845	.0308	.0000	.0048	.2919	.0561
O ₂₉	.845 < Y ≤ .894	.0078	.0000	.0018	.1237	.0423
O ₃₀	.894 < Y ≤ .957	.0012	.0000	.0005	.0138	.0337
O ₃₁	.957 < Y ≤ 1.00	.0000	.0000	.0001	.0001	.0109

5. ASYMPTOTIC PERFORMANCE OF THE PROPOSED METHOD

The performance of the proposed method depends on the estimation procedure that is used. Here, we will consider estimation of various percentiles of the response curve by using linear combinations of the maximum likelihood estimators of μ and σ . Maximum likelihood is often used to estimate location and scale parameters in problems with censored data (see e.g., Nelson 1982, and Lawless 1982). There are a number of computer codes that can produce maximum likelihood estimators from censored data (see e.g., CENSOR authored by Meeker and Duke 1979, and PROC LIFEREG produced by the SAS Institute 1988).

With relatively weak regularity conditions (which are met here), maximum likelihood estimators are asymptotically (with respect to n) normally distributed (see e.g., Serfling 1980). Specifically in the case of estimating μ ,

$$\sqrt{n}(\hat{\mu}_n - \mu) \xrightarrow{\mathcal{L}} \text{Normal}\left(0, \frac{1}{I_F(\mu)}\right) \text{ as } n \rightarrow \infty, \text{ where} \quad [5.1]$$

$\hat{\mu}_n$ is the m.l.e. and $I_F(\mu)$ is the Fisher Information with respect to μ . In our example,

$$I_F(\mu) = - \sum_{m=1}^{31} P_{\infty}(O_m; \mu, \sigma) \frac{\partial^2 L(O_m)}{\partial \mu^2},$$

where $L(O_m)$ is the log-likelihood that the threshold energy is consistent with the m^{th} outcome. For instance, $L(O_1) = \log\left(\Phi\left\{\frac{.400 - \mu}{\sigma}\right\}\right)$, $L(O_{10}) = \log\left(1 - \Phi\left\{\frac{.620 - \mu}{\sigma}\right\}\right)$, and $L(O_{19}) = \log\left(\Phi\left\{\frac{.450 - \mu}{\sigma}\right\} - \Phi\left\{\frac{.400 - \mu}{\sigma}\right\}\right)$ are the log-likelihoods associated with certain left-censored, right-censored, and interval-censored observations, respectively.

In order to describe the asymptotic performance of the method/estimator, one can evaluate $\frac{1}{I_F(\mu)}$ over the range of interest for μ and σ . Furthermore, one can easily compute the asymptotic relative efficiency of the method/estimator with respect to the maximum likelihood estimator based on complete data. By complete data, we mean the actual threshold energy for every pellet tested is observed. The asymptotic relative efficiency is then the ratio of the variance of \bar{Y} , the sample mean of a complete data set, to the variance of $\hat{\mu}$, and is given by A.R.E. $(\hat{\mu} | \mu, \sigma) = \sigma^2 I(\mu)$. Figure 4 shows (roughly) how the A.R.E. of $\hat{\mu}$ varies over the region of interest. Figure 4 provides a clear indication that the proposed method estimator is relatively efficient for estimating μ . Note that, among those points considered in the $\{\mu, \sigma\}$ plane, the A.R.E. of $\hat{\mu}$ is highest when $\mu = .7$ Joules and $\sigma = .05$ Joules. This occurs because: 1. $\mu = .7$ Joules splits the range of stimulus levels and, 2. $\sigma = .05$ Joules is close to the typical step size between successive stimulus levels. With regard to 1., as μ moves away from .7 Joules, the A.R.E. of $\hat{\mu}$ decreases because the likelihood of relatively noninformative single-censored outcomes (either left or right censored) increases. With regard to 2., others (e.g., Davis 1971) have found that the up-and-down method is most efficient when

$\sigma \approx \Delta$ (the step size). Note that the particular configuration of stimulus levels leads to discontinuities and minor features in A.R.E. $(\hat{\mu} | \mu, \sigma)$ that are not apparent in Figure 4.

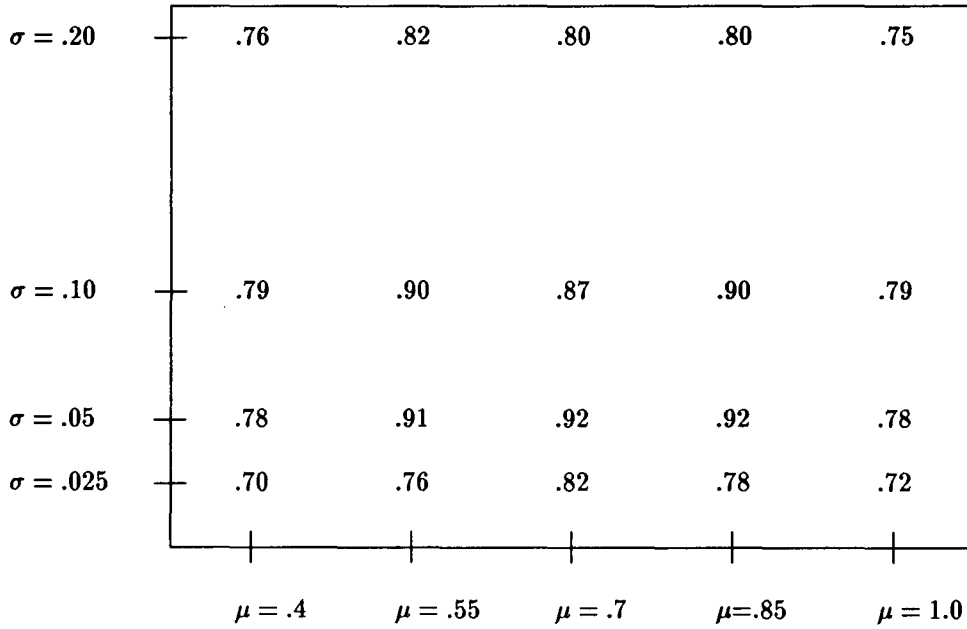


Figure 4 - Asymptotic Relative Efficiency (A.R.E.) of $\hat{\mu}$ for Various Values of μ and σ

An analogous technique can be used to compute the asymptotic performance of the method when the objective is to estimate an arbitrary percentile of the energy threshold distribution with $\hat{\mu} + z_p \hat{\sigma}$, where z_p is the p^{th} percentile of the standard normal distribution. For arbitrary p , as $n \rightarrow \infty$,

$$\sqrt{n} \left(\hat{\mu} + z_p \hat{\sigma} - (\mu + z_p \sigma) \right) \xrightarrow{\mathcal{L}} \text{Normal}(0, \Sigma) \text{ as } n \rightarrow \infty, \text{ where} \quad [5.2]$$

$\Sigma = (z_p, 1) (\mathbf{I}_F)^{-1} (z_p, 1)^T$, and

$$\mathbf{I}_F = \begin{bmatrix} I_F(\sigma, \sigma) & I_F(\mu, \sigma) \\ I_F(\mu, \sigma) & I_F(\mu, \mu) \end{bmatrix}, \text{ is the Fisher Information Matrix.}$$

$$I_F(\sigma, \sigma) = - \sum_{m=1}^{31} P_{\infty}(O_m; \mu, \sigma) \frac{\partial^2 L(O_m)}{\partial \sigma^2},$$

$$I_F(\mu, \mu) = - \sum_{m=1}^{31} P_{\infty}(O_m; \mu, \sigma) \frac{\partial^2 L(O_m)}{\partial \mu^2}, \text{ and}$$

$$I_F(\mu, \sigma) = - \sum_{m=1}^{31} P_{\infty}(O_m; \mu, \sigma) \frac{\partial^2 L(O_m)}{\partial \mu \partial \sigma}.$$

See the appendix regarding expressions for $\frac{\partial^2 L(O_m)}{\partial \sigma^2}$, $\frac{\partial^2 L(O_m)}{\partial \mu^2}$, and $\frac{\partial^2 L(O_m)}{\partial \mu \partial \sigma}$.

In the case of the battery heat pellets, the 90th percentile (P_{90}), is of special interest to the production engineers. Figure 5 shows how the A.R.E. of $\hat{P}_{90} = \hat{\mu} + 1.28 \cdot \hat{\sigma}$ varies

over the region of interest. In general, the A.R.E. of \hat{P}_{90} decreases from low to high values of μ (especially for large values of σ). The relatively poor asymptotic behavior of \hat{P}_{90} at $\mu = 1$ is due to the fact that the errors in $\hat{\mu}$ and $\hat{\sigma}$ are *positively* correlated when μ is near 1. In contrast, the errors in $\hat{\mu}$ and $\hat{\sigma}$ are *negatively* correlated when μ is near .4 (A.R.E. is highest here). With regard to σ , there is some indication that the A.R.E. of this method/estimator is best when σ is close to the typical difference between successive stimulus levels ($\approx .05$). In addition, there seems to be a localized area ($\mu = .4$ and $\sigma = .025$) where \hat{P}_{50} (see Figure 4) and \hat{P}_{90} are somewhat inefficient due to the substantial likelihood of left censoring.

$\sigma = .20$.72	.50	.42	.38	.25
$\sigma = .10$.86	.73	.65	.67	.33
$\sigma = .05$.80	.88	.83	.82	.33
$\sigma = .025$.52	.81	.67	.65	.30
	$\mu = .4$	$\mu = .55$	$\mu = .7$	$\mu = .85$	$\mu = 1.0$

Figure 5 - Asymptotic Relative Efficiency (A.R.E.) of \hat{P}_{90} for Various Values of μ and σ

6. MONTE CARLO SIMULATIONS

Although we have derived the asymptotic performance of the proposed method when maximum likelihood is used to estimate μ and σ , it is of interest to characterize the method's performance for relatively small samples. A limited simulation study was conducted for this purpose, with $n = 20$. The performance of the proposed method, over various combinations of μ and σ , was examined (see Tables 3 and 4). RANNOR (SAS Institute 1988) was used to generate one hundred realizations of 20 random normal variates for each combination of μ and σ that was considered. Note that if n is relatively small, the efficiency of the method depends to a degree on where μ is relative to the initial position of the testing window. In the simulations discussed here, this

position was fixed at $S_1^1 = R_5 = .589$ Joules (i.e., the initial stimulus applied to the first of the 20 pellets in sample).

For each sample set, PROC LIFEREG (SAS Institute 1988) was used to provide $\hat{\mu}$ and $\hat{\sigma}$ and an estimated covariance matrix for these parameter estimates. Tables 3 and 4 summarize the 100 sample values of the estimated 50th and 90th percentiles of the response curves ($\hat{P}_{50} = \hat{\mu}$ and $\hat{P}_{90} = \hat{\mu} + 1.28\hat{\sigma}$) for each combination of μ and σ that is given. In several instances (associated with small values of σ), PROC LIFEREG was unable to return estimates of μ and σ due to a heavy concentration of results in one or two censoring intervals. In these cases, additional realizations were performed so that 100 sample values of $\hat{\mu}$ and $\hat{\sigma}$ were available for each combination of μ and σ . The total number of realizations needed to provide 100 sample values of $\hat{\mu}$ and $\hat{\sigma}$ (r^*) is reported in Table 3. Note also that the conditions summarized in Tables 3 and 4 do not cover the complete range of parameters portrayed in Figures 4 and 5. In *many* instances, with extreme μ (.4 or 1.0) and small σ (.025 or .05), PROC LIFEREG was not able to return estimates of μ and σ due to the previously described problem. This problem is further aggravated due to the preponderance of poor quality left(right)-censored results (relative to interval-censored results) in these situations.

The accuracies of \hat{P}_{50} and \hat{P}_{90} can be assessed by comparing the column of sample means in Tables 3 and 4 with the appropriate linear combination of μ and σ . From these comparisons it is evident that \hat{P}_{50} and \hat{P}_{90} are reasonably accurate over the various combinations of μ and σ considered here. The efficiencies of \hat{P}_{50} and \hat{P}_{90} , relative to those of the corresponding percentile estimates based on the known complete data (\bar{X} and $\bar{X} + 1.28 \cdot S$), are given by R.E. in Tables 3 and 4. In general, there is good agreement between the values of A.R.E. (from Figures 4 and 5) and the sample values of R.E. With $n = 20$ and for extreme values of μ (.4 and 1.0), the A.R.E. is an optimistic predictor of the sample R.E., due in part to the distance from μ to the initial testing window.

Table 3 - Summary of Simulation Results for \hat{P}_{50} by μ and σ

A.R.E. = asymptotic efficiency of \hat{P}_{50} relative to \bar{X} with complete data

R.E. = sample efficiency of \hat{P}_{50} relative to \bar{X} with complete data

r* = number of realizations needed to provide 100 sample values of \hat{P}_{50}

μ	σ	Sample Mean	Sample Std. Dev.	A.R.E.	R.E.	r*
.40	.1	.394	.036	.79	.42	100
.40	.2	.389	.069	.76	.50	100
.55	.025	.550	.0057	.76	.69	104
.55	.05	.549	.0113	.91	.84	102
.55	.1	.551	.023	.90	.91	100
.55	.2	.546	.060	.82	.58	100
.70	.025	.700	.0060	.82	.80	100
.70	.05	.701	.0106	.92	.98	102
.70	.1	.702	.022	.87	.85	100
.70	.2	.696	.046	.80	.93	100
.85	.025	.849	.0065	.78	.77	104
.85	.05	.851	.0110	.92	.89	100
.85	.1	.847	.025	.90	.76	100
.85	.2	.853	.059	.80	.51	100
1.00	.1	1.003	.028	.79	.59	103
1.00	.2	1.013	.072	.75	.34	100

Table 4 - Summary of Simulation Results for \hat{P}_{90} by μ and σ

A.R.E. = asymptotic efficiency of \hat{P}_{90} relative to \bar{X} with complete data

R.E. = sample efficiency of \hat{P}_{90} relative to \bar{X} with complete data

μ	σ	P_{90}	Sample Mean	Sample Std. Dev.	A.R.E.	R.E.
.40	.1	.528	.522	.033	.86	.79
.40	.2	.656	.646	.077	.72	.60
.55	.025	.582	.579	.0097	.81	.59
.55	.05	.614	.609	.0141	.88	.94
.55	.1	.678	.677	.036	.73	.80
.55	.2	.806	.809	.028	.50	.53
.70	.025	.732	.731	.0094	.67	.61
.70	.05	.764	.762	.0147	.83	.99
.70	.1	.828	.828	.037	.65	.53
.70	.2	.956	.943	.107	.42	.35
.85	.025	.882	.876	.0142	.65	.29
.85	.05	.914	.912	.0157	.82	.84
.85	.1	.978	.976	.041	.67	.58
.85	.2	1.106	1.108	.117	.38	.31
1.00	.1	1.128	1.128	.058	.33	.25
1.00	.2	1.256	1.288	.188	.25	.11

The estimated covariance matrix of $(\hat{\mu}, \hat{\sigma})$, provided by PROC LIFEREG, can be used to develop approximate confidence intervals for P_{50} and P_{90} . For example, an approximate central confidence interval for P_{50} with coverage $(1-\alpha)$ is given by

$$\hat{P}_{50} \pm z_{\frac{\alpha}{2}} \cdot \sqrt{\hat{\text{Var}}(\hat{\mu})}. \quad [6.1]$$

Similarly, an approximate confidence interval for P_{90} with coverage $(1-\alpha)$ is given by

$$\hat{P}_{90} \pm z_{\frac{\alpha}{2}} \cdot \sqrt{\hat{\text{Var}}(\hat{\mu}) + (1.28)^2 \cdot \hat{\text{Var}}(\hat{\sigma}) + 2 \cdot 1.28 \cdot \hat{\text{Cov}}(\hat{\mu}, \hat{\sigma})}. \quad [6.2]$$

The quality of these confidence intervals can be evaluated by considering the distributions of $\Delta_{50} = \frac{\hat{P}_{50} - P_{50}}{\sqrt{\hat{\text{Var}}(P_{50})}}$ and $\Delta_{90} = \frac{\hat{P}_{90} - P_{90}}{\sqrt{\hat{\text{Var}}(P_{90})}}$ for the various simulation conditions considered. Figures 6 and 7 display summaries of these distributions.

From Figure 6, it is apparent that eqn. 6.1 provides useful confidence intervals for P_{50} for levels of α at least as small as .2 (i.e., the 10th and 90th percentiles of Δ_{50} are consistent with $\Phi^{-1}(.1)$ and $\Phi^{-1}(.9)$, respectively. However, in the case of Δ_{90} (see Figure 7), it is apparent that eqn. 6.2 provides confidence intervals with poorer quality than those produced by eqn. 6.1. In general, the distributions of Δ_{90} are skewed significantly to the left. This is due to the non-normal, asymmetric nature of the distribution of $\hat{\sigma}$ which causes the distribution of \hat{P}_{90} to deviate from normality. In general, the result is that lower α -level confidence limits for \hat{P}_{90} , constructed via eqn 6.2, will be *conservative*, while upper α -level confidence limits for \hat{P}_{90} will be *anticonservative* (i.e., $\text{Prob}\{P_{90} \geq \hat{P}_{90} + \Phi^{-1}(.90) \cdot \sqrt{\hat{\text{Var}}(P_{90})}\} \geq .1$). Note that this problem will be exacerbated when constructing confidence intervals for more extreme percentiles when using the approach illustrated by eqn. 6.2. Thus, with regard to evaluating production lots of heat pellets, lot acceptance based on α -level upper confidence limits for P_{90} will result in consumer's risk that is somewhat larger than α .

In summary, the estimates of P_{50} and P_{90} using the proposed method/estimator were shown to be both accurate and relatively efficient for samples of size $n = 20$. Furthermore, useful confidence regions for P_{50} and P_{90} can be obtained by using eqn.'s 6.1 and 6.2 in conjunction with the asymptotic covariance estimates of $\hat{\mu}$ and $\hat{\sigma}$ provided by PROC LIFEREG.

7. CONCLUSION

A simple strategy for evaluating the ignition sensitivity of thermal battery heat pellets has been proposed. The strategy has been shown (both asymptotically and through simulation) to be relatively efficient in terms of the number of pellets to be tested. The high efficiency of the proposed method seems to be at odds with the fact that the data are incomplete. The basis for the relatively good efficiency of this strategy is the conversion of relatively uninformative left(right)-censored outcomes to interval-censored outcomes. One could, in principal, improve this method by using intermediate estimates of μ and σ to set the conditions of subsequent testing. However, due to the relatively good efficiency of the proposed method, the efficiency gain would be minimal, at best.

ACKNOWLEDGEMENTS

I thank Kathleen Diegert, Bob Easterling and Ron Guidotti for suggestions that helped the presentation of this material.

REFERENCES

- Davis, M. (1971), "Comparison of Sequential Bioassays in Small Samples," *Journal of the Royal Statistical Society, Series B*, 33, 78-87.
- Dixon, W. J. and Mood, A. M. (1948), "A Method for Obtaining and Analyzing Sensitivity Data," *Journal of the American Statistical Association*, 43, 109-126.
- Isaacson, D. L. and Madsen, R. W. (1976), *Markov Chains: Theory and Applications*, New York: John Wiley.
- Lawless, J. F. (1982), *Statistical Models and Methods for Lifetime Data*, New York: John Wiley.
- Meeker, Jr., W. Q. and Duke, S. (1979), "CENSOR - A User-Oriented Computer Program for Life Data Analysis," Department of Statistics, Iowa State University, Ames Iowa.
- Nelson, W. (1982), *Applied Life Data Analysis*, New York: John Wiley.
- Robbins, H. and Monro, S. (1951), "A Stochastic Approximation Method," *Annals of Mathematical Statistics*, 29,400-407.
- SAS Institute Inc. (1988), *SAS/STAT™ User's Guide, Release 6.03 Edition*, Cary, NC: SAS Institute Inc.
- Serfling, Robert J. (1980), *Approximation Theorems of Mathematical Statistics*, New York: John Wiley.
- Vincent, C. A., Scrosati B., Lazzari, M., Bonino, F. (1984), *Modern Batteries*, London, Edward Arnold Publishers.
- Wu, C. F. Jeff (1985), "Efficient Sequential Designs With Binary Data," *Journal of the American Statistical Association*, 80, 974-984.

APPENDIX - Expressions for $\frac{\partial^2 L(O_m)}{\partial \sigma \partial \sigma}$, $\frac{\partial^2 L(O_m)}{\partial \mu \partial \mu}$, and $\frac{\partial^2 L(O_m)}{\partial \mu \partial \sigma}$.

$$\frac{\partial^2 L(O_m)}{\partial \sigma^2} = \frac{1}{\sigma^2} \left\{ \frac{z_U^2 \phi'(z_U) - z_L^2 \phi'(z_L) + 2\{z_U \phi(z_U) - z_L \phi(z_L)\}}{\Phi(z_U) - \Phi(z_L)} - \frac{\{z_U \phi(z_U) - z_L \phi(z_L)\}^2}{\{\Phi(z_U) - \Phi(z_L)\}^2} \right\}.$$

$$\frac{\partial^2 L(O_m)}{\partial \mu^2} = \frac{1}{\sigma^2} \left\{ \frac{\phi'(z_U) - \phi'(z_L)}{\Phi(z_U) - \Phi(z_L)} - \frac{\{\phi(z_U) - \phi(z_L)\}^2}{\{\Phi(z_U) - \Phi(z_L)\}^2} \right\}.$$

$$\frac{\partial^2 L(O_m)}{\partial \mu \partial \sigma} = \frac{1}{\sigma^2} \left\{ \frac{z_U \phi'(z_U) - z_L \phi'(z_L) + \phi(z_U) - \phi(z_L)}{\Phi(z_U) - \Phi(z_L)} - \frac{(\phi(z_U) - \phi(z_L))(z_U \phi(z_U) - z_L \phi(z_L))}{\{\Phi(z_U) - \Phi(z_L)\}^2} \right\}.$$

z_U (z_L) defines the upper (lower) censoring limit in terms of a standard normal variable, $\phi(\cdot)$ is the standard normal density function, and $\Phi(\cdot)$ is the standard normal cumulative distribution function. For left-censored outcomes, $z_L = -\infty$. For right-censored outcomes, $z_R = +\infty$. Note that $\Phi(-\infty) = 0$, $\Phi(+\infty) = 1$, $\phi(-\infty) = 0$, $\phi(+\infty) = 0$, $\phi'(-\infty) = 0$, and $\phi'(+\infty) = 0$.

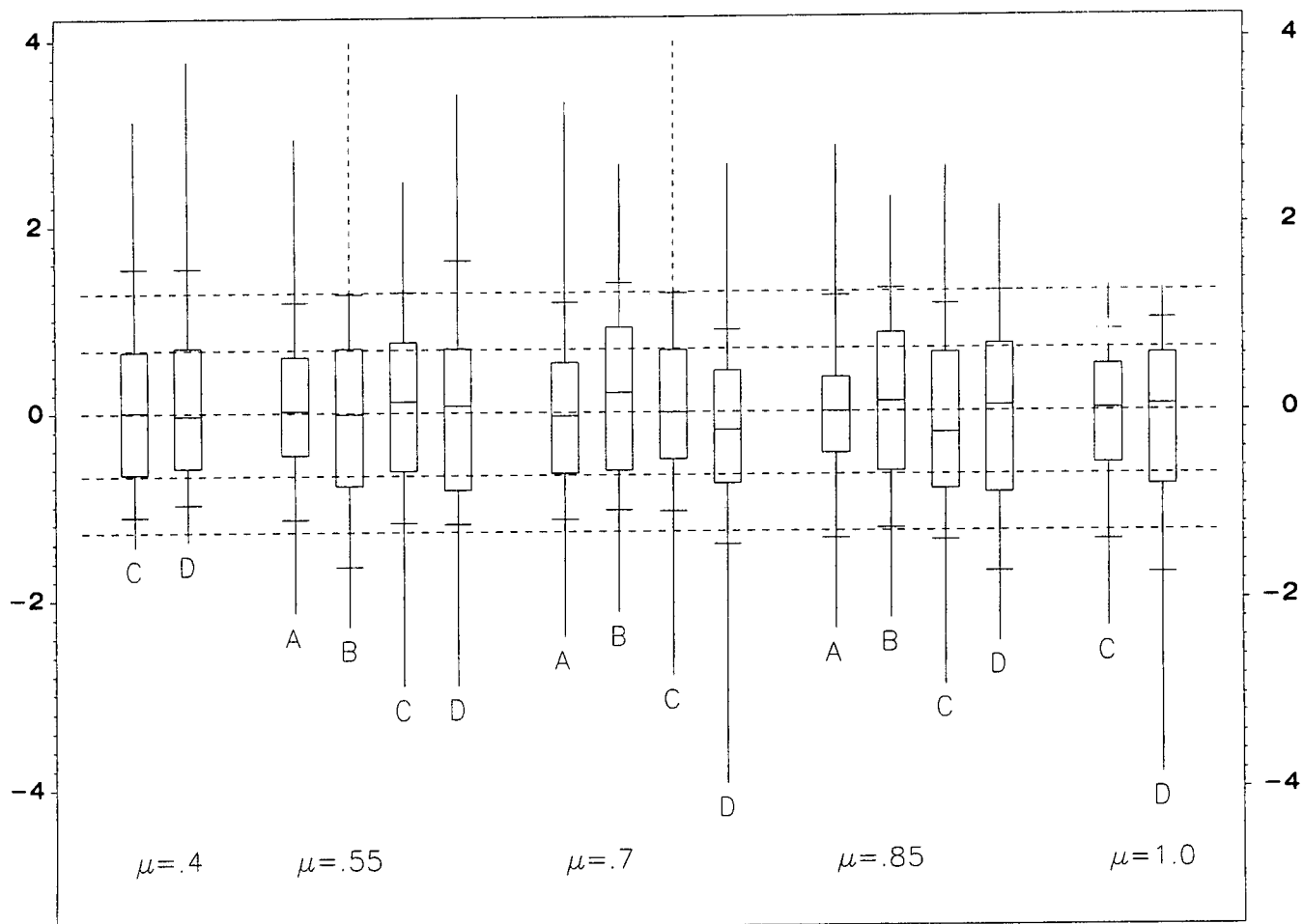


Figure 6 - Distributions of $\Delta_{50} = \frac{\hat{P}_{50} - P_{50}}{\sqrt{\hat{\text{Var}}(P_{50})}}$ for the various simulation conditions indexed by $\mu \in \{.4, .55, .7, .85, 1.0\}$ and $\sigma \in \{.025 \text{ (A)}, .05 \text{ (B)}, .1 \text{ (C)}, .2 \text{ (D)}\}$. In addition to the minimum and maximum (when offscale denoted by a broken line), the 10th, 25th, 50th, 75th, and 90th percentiles are displayed. Horizontal broken lines are displayed at the following levels: $\Phi^{-1}(.10) = -1.28$, $\Phi^{-1}(.25) = -.674$, 0 , $\Phi^{-1}(.75) = .674$, $\Phi^{-1}(.90) = 1.28$.

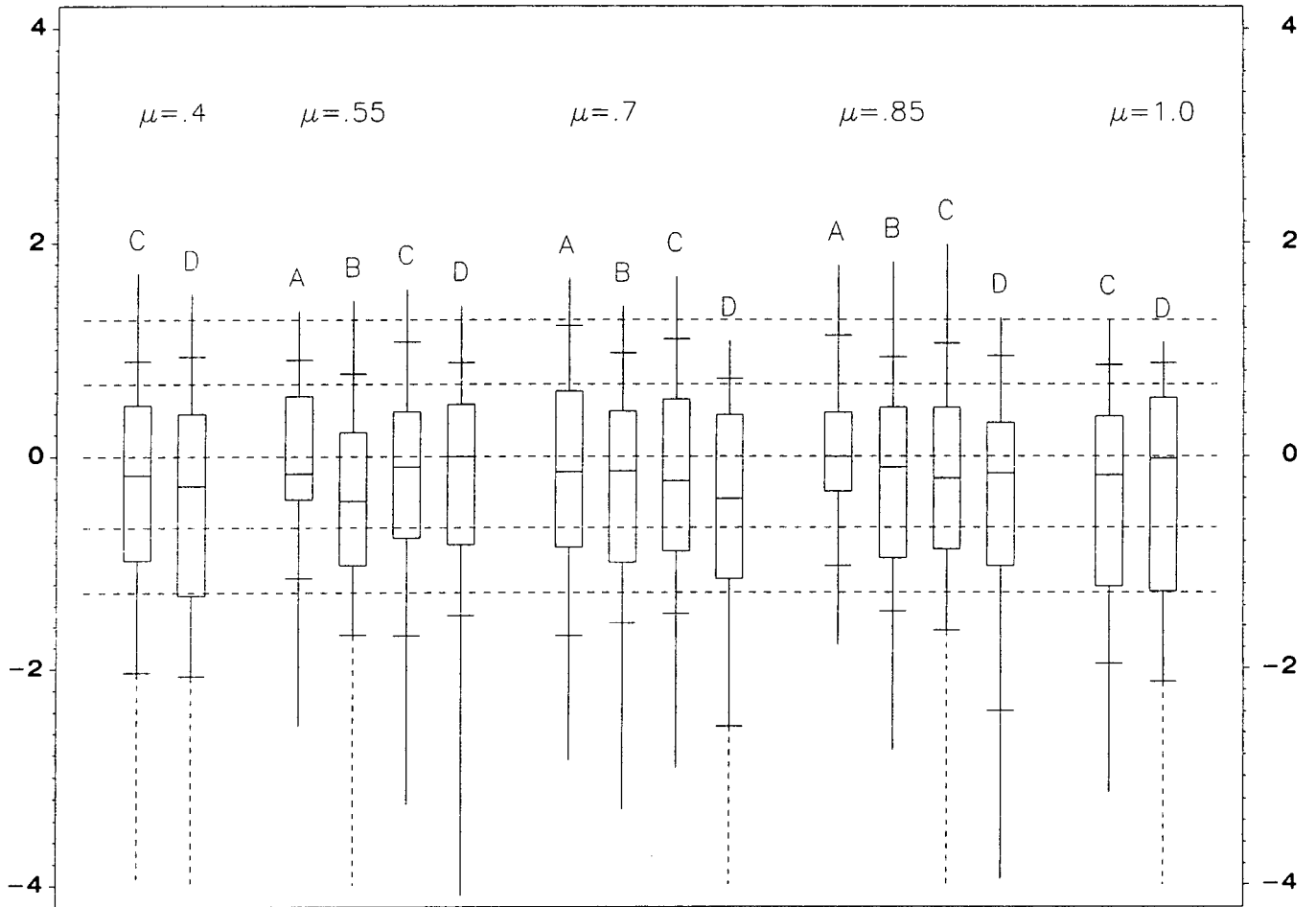


Figure 7 - Distributions of $\Delta_{90} = \frac{\hat{P}_{90} - P_{90}}{\sqrt{\hat{\text{Var}}(P_{90})}}$ for the various simulation conditions

indexed by $\mu \in \{.4, .55, .7, .85, 1.0\}$ and $\sigma \in \{.025 \text{ (A)}, .05 \text{ (B)}, .1 \text{ (C)}, .2 \text{ (D)}\}$.

SNL DISTRIBUTION:

323	S. V. Crowder
323	K. V. Diegert
323	R. G. Easterling
323	L. L. Halbleib
323	K. M. Hansen
323	B. M. Rutherford
323	D. D. Sheldon
323	F. W. Spencer
323	E. V. Thomas (20)
2512	J. A. Merson
2512	R. R. Weinmaster
2513	R. W. Bickes
2522	J. A. Gilbert
2522	K. R. Grothaus
2522	R. A. Guidotti
2522	G. L. Scharrer
7141	Technical Library (5)
7151	Technical Publications
7613-2	Document Processing for DOE/OSTI (10)
8523-2	Central Technical Files

SPECIFIED EXTERNAL DISTRIBUTION:

EG&G Mound
Attn: Larry Dosser
P. O. Box 32
Miamisburg, OH 45343-0987

Eagle-Picher Industries, Inc. (7)
Electronics Div. Couples Dept.
Attn: R. Cottingham
R. Spencer
F. Smith
J. DeGruson
R. Hudson
J. Harvel
J. Owen
P. O. Box 47
Joplin, MO 64802

Harry Diamond Labs
Attn: J. T. Nelson
2800 Powder Mill Road
Adelphi, MD 20783

Naval Surface Warfare Center
Attn: C. Winchester
Code R33
10901 New Hampshire Ave.
Silver Spring, MD 20903-5000

Royal Aerospace Establishment (3)
Materials Dept.
Attn: A. Attewell
I. Faul
J. Knight
Farnborough, ENGLAND

SAFT America (3)
Attn: K. K. Press
J. D. Briscoe
J. Embry
107 Beaver Court
Cockeysville, MD 21030

Unidynamics/Phoenix
Attn: J. Fronabarger
P. O. Box 46100
Phoenix, AZ 85036-6100